

Common pathways and functional profiles reveal underlying patterns in Breast, Kidney and Lung cancers

Sergio Romera-Giner

Atos

Francisco García-García

Centro de Investigacion Principe Felipe

Marta Hidalgo (✉ mhidalgo@cipf.es)

Centro de Investigacion Principe Felipe <https://orcid.org/0000-0002-5801-7804>

Research

Keywords: cancer, signaling, pathways, functional analysis, common

Posted Date: February 29th, 2020

DOI: <https://doi.org/10.21203/rs.3.rs-15503/v1>

License:  This work is licensed under a Creative Commons Attribution 4.0 International License.

[Read Full License](#)

Version of Record: A version of this preprint was published at Biology Direct on May 26th, 2021. See the published version at <https://doi.org/10.1186/s13062-021-00293-8>.

Abstract

Background : Cancer is an extremely heterogeneous disease, both intra and inter cancer types. In this work we aim to establish common patterns in Breast, Kidney and Lung cancers at the signaling pathways and functional level which give rise to the generic microenvironment of cancer, as well as determine cancer-specific pathways and functions related to each disease.

Results : After a tumor vs. normal tissue comparison of the levels of activation of the signaling pathways and cell functions, we found a significant number of common subpathways and functions related to the three studied tumors. Also common survival mechanisms were established. Cancer-specific features which are only significant in one of the tumors have been determined.

Conclusions : The joint analysis of these different cancer datasets reported an appreciable number of common functional features, some of them related at the same time to survival in two of the three analyzed cancers. On the other hand, tumor-specific subpathways and functions have been determined, allowing a better understanding of the specificity of each cancer. **Keywords :** cancer, signaling, pathways, functional analysis, common

Background

Due to complex factors as aging and population growth, cancer incidence and mortality are rapidly growing worldwide. Nowadays, cancer is one of the major causes of death in most countries at ages below 70 years according to the World Health Organization (WHO), with lung cancer being the leading cause of cancer death in both sexes [1].

Cancer is an extremely heterogeneous disease, both intra and inter cancer types. Even patients with the same cancer may be classified in different subtypes according to the specific characteristics of each tumor. Also, the diverse tissues or even cell types of origin define a set of specific features linked to each cancer which characterize them. However, distinct types of cancer, despite origin differences and derived specific features, share a list of common underlying patterns, known as hallmarks [2]. These hallmarks are a set of basic functionalities that the cell must acquire to become carcinogenic and include features as growth suppressors evasion, the activation of tissue invasion and metastasis or the resistance to cell death mechanisms. As cancer research advances, new biological capabilities emerge as hallmarks, such as evasion of immune destruction and reprogramming cell energy metabolism [3].

In the last years, mainly due to the decrease in the cost of the sequencing techniques and the popularization of bioinformatics methods, the analysis of the genomic and transcriptomic data of patients has become a growing approach to the study of cancer [4,5]. It is widely known that specific

mutations are able to induce cancer [4] and that many genes and microRNAs are deregulated in tumor tissues [5]. The study of the genomic characteristics of each cancer has led to the establishment of diverse subtypes defined by the different mutations they include and with a very heterogeneous response to drugs and survival [6]. To address the differences between these subtypes, many bioinformatic approaches have been developed, such as CancerSubtypes, a R package aimed to retrieve all the main computational methods for cancer subtypes identification and analysis [7].

In the past, many of the approaches followed to analyze cancer data in Bioinformatics were based in the analysis of genes individually. However, genes do not work alone, but in combination with many other genes in what can be understood as a network of interactions. In particular, signaling pathways emerge as an important cell mechanism which allow cells to respond to external stimuli and are at the core of many cell deregulation patterns which lead to different diseases [8,9].

The study of signaling pathways in the context of cancer has proven to give interesting results both in determining the mechanisms of the diseases and in the prediction of survival time [10,11]. The tool Hipathia [12] has recently demonstrated its ability to detect differentially activated subpathways while keeping a very low False Positive Rate, outperforming many other signaling pathway tools [13].

With the massive amount of data being generated around the world as a result of cancer analysis every day, one of the main aims of cancer bioinformatics is to manage and integrate this information in an understandable way. Cancer data clouds, such as The Cancer Genome Atlas (TCGA) [14] or The Cancer Imaging Archive (TCIA) [15] are one of the resources that allow researchers to manage large amounts of datasets and to keep track of the changes. Integration of the existing data has become also mandatory to interpret the results with a global perspective.

In this context, the CAMDA 2019 Hi-Res Cancer Data Integration Challenge aims to develop and demonstrate novel methods for gaining novel biological insights or improving support for Precision Medicine. In this work we aim to establish common patterns at the signaling pathways level which, beyond specific differences due to the tissue of origin, give rise to the generic microenvironment of cancer in breast, lung and kidney tissues. At the same time, we aim to determine the cancer-specific signaling pathways which define the particular features of each disease.

Results

Tumor vs. normal tissue comparisons

The datasets were downloaded and processed as described in methods, and the comparison of tumor vs. normal samples for the levels of activity of the pathways and functions analyzed were applied accordingly. The comparison of the different activities at the subpathway and functional level between tumor and healthy tissue samples returned the number of up- and down-activated significant features in each project shown in Table 1.

Number of significant results per project and feature

| | Paths | | | Gene Ontology | | | Uniprot | | |
|-------------|-------|------|-------|---------------|------|-------|---------|------|-------|
| | UP | DOWN | TOTAL | UP | DOWN | TOTAL | UP | DOWN | TOTAL |
| BRCA | 483 | 819 | 1302 | 388 | 848 | 1236 | 32 | 93 | 125 |
| KIRC | 805 | 635 | 1440 | 804 | 541 | 1345 | 51 | 65 | 116 |
| LUAD | 386 | 925 | 1311 | 242 | 1165 | 1407 | 27 | 96 | 123 |

Table 1: Number of significant features per project and analyzed feature. For each feature type, the number of significant up-activated, down-activated and total significant features is shown.

The significant subpathways as defined in methods for each project are depicted as heatmaps in Figure 1. Samples and features were clusterized, and clear patterns emerged from the clusterization in all three projects, allowing easily the separation between tumor and normal samples just from the values of pathway activity.

The clear pattern between tumor and normal samples is also perceptible in the heatmaps of the functional activities, proving a notable capacity of the functional data to discern between both groups, see Figure 2.

Common & specific features

After comparing tumor and normal samples separately, we looked for the features with a common pattern of significant up- or down-activation across the three cancers. We found 431 common subpathways, 400 common Gene Ontology functions and 52 common Uniprot functions, representing 23%, 24% and 36% of the total number of analyzed features, respectively.

Common pathways include subpathways from the Cell cycle (up-activated subpathways ending in RB1 and protein complexes including MCM and ORC families), Toll-like receptor signaling pathway (up-activated subpathways ending in proteins CXCL9, CXCL10, CXCL11, IFNB1, related to angiogenesis), Hippo signaling pathway (down-activated subpathways ending in ID1, NKD1 or CTGF), MAPK signaling pathway (down-activation of subpathways ending in NR4A1 and MAP3K4, which are reportedly tumor suppressors, and up-activation of subpathways ending in ELK1, TP53 and CDC25B, with oncogenic properties), PPAR signaling pathway (down-activation of subpathways ending in proteins AQP7, GK, PCK1, ACAA1, CPT1C, ACSL1, LPL, SLC27A4, strongly related to lipid and fatty acid metabolisms), ERBB signaling pathway (subpathways ending in proteins CDKN1A, CDKN1B, BAD, GSK3B, EIF4EBP1 are up and those ending in RPS6KB1, STAT5A and PRKCA are down) and AMPK signaling pathway. Supplementary Tables S1, S2 and S3 in supplementary material show the list of common pathways, GO terms and Uniprot keywords, respectively, their common status and the *p-values* of the comparisons between tumor and normal samples in each of the projects, ordered by the sum of the three *p-values*.

Interestingly, when analyzing differential expression of the genes involved in those paths, specific cancer patterns arise. As an example, Figure 3A (top) shows the boxplots representing the distribution of the subpathway *AMPK signaling pathway: CCNA2* (the subpathway from the KEGG *AMPK signaling pathway* with effector protein CCNA2) in tumor and normal samples for each of the projects. A common pattern of up-activation is clear. Figure 3B shows the Hipathia visualization for the same subpathway for the tumor vs. normal comparisons in BRCA (top), LUAD (center) and KIRC (bottom), including gene differential expression. Notice that just two of the twelve involved nodes present a common differentially expressed pattern among all three cancers and yet the joint subpathway activity presents the same behaviour in all of them.

Going further the expected GO terms usually found in cancer and that we found in our analysis, such as the histones H3 and H4 methylation and acetylation, DNA replication and recombination, we can see an interesting mix of up and down regulated functions that can be related to cancer hallmarks. Common upregulated GO functions, such as the regulation of adaptive immune response, the leukocyte migration, and the ones related to T cell activation and B cells apoptosis hint the complex relation that these kind of immune system cells have with tumors [16] and the cancer hallmark of evading immune suppression. Also, we can observe an upregulated JAK-STAT cascade, strongly related to cell survival, migration and proliferation, making this signaling pathway an important indicator of tumorigenesis and, by definition, an important indicator of hallmarks of cancer such as the activation of invasion and metastasis and sustaining proliferative signaling.

On the other hand, with respect to downregulated GO terms, we find certain functions, such as glucose homeostasis DNA repair processes, that could be related to the hallmarks deregulation of cell energetics and genome instability and mutation respectively. Also, a great number downregulated GO terms are related to the ion levels of the cell, such as sodium export and import from cell, response to calcium ion, regulation of delayed rectifier potassium channel activity or the regulation of intracellular pH. The varying levels of different kinds of ions is oftenly related to changes in the expression levels of ion channeling proteins, which can be related to identify different kinds of cancer and their severity [17].

With respect to the common Uniprot keywords, significant functions include Mitosis (up-activated, see Figure 3A, bottom), Growth arrest (down-activated), Lipid degradation (down-activated), calcium transport (down-activated), Porin (up-activated) and Chromosome partition (up-activated), which, respectively, can be related to hallmarks Enabling replicative immortality, Evading growth suppressors, Deregulating cellular energetics, Sustaining proliferative signaling, Activating invasion and metastasis and Genome instability and mutation.

Also an interesting number of cancer-specific features arise from the analysis. Concretely, Figure 4A shows the number of specific subpathways and functions for each of the projects. The most specific cancer seems to be KIRC, with the greatest number of specific subpathways and functions differentially activated.

Specific subpathways related to KIRC include the up-activated Hippo signaling pathway (ending in protein BBC3) and also the up-activated TNF signaling pathway (ending in proteins CASP7, CASP3, CEBPB, CHUK, MAPK14 and PGAM5). Specific Uniprot functions include the up-activation of Ubl conjugation pathway and complement pathway and specific Gene Ontology terms include down-activation of carnitine transport, up-activation of the regulation of cell adhesion mediated by integrin and up-activation of substrate adhesion-dependent cell spreading.

With respect to BRCA, specific Gene Ontology terms include the up-activated longevity regulating pathway (ending in proteins SOD2, CAT and ATCG5) and the up-activated adherens junction pathway (ending in proteins LEF1, CTNNB1, and CTNND1). Just one Uniprot function has been found to be specific to BRCA: the down activation of B-cells. And for the part of specific Gene Ontology terms, we could see functions such as the up-activation of the hydrogen peroxide biosynthetic process and the down-activation of apoptotic cell clearance.

Finally, LUAD specific pathway results include the down-activated apoptosis pathway (ending in protein PTPN13) and the up-activated thyroid hormone signaling pathway (ending in the protein CASP9). Again, just one Uniprot function specific to LUAD has been found, the up-activation of necrosis. Finally, specific Gene Ontology terms for LUAD include the up-activation of cytokine biosynthetic process and the up-activation of cation transport.

Supplementary Tables S4, S5 and S6 include the cancer specific subpathways, GO terms and Uniprot keywords, together with the sign of the comparison and the project in which they were significant.

Survival-related pathways and functions

After applying the survival pipeline explained in Methods, we found the number of pathways and functions related to survival depicted in Table 2.

Number of significant survival-related features per project

| | Paths | Gene Ontology | Uniprot |
|-------------|-------|---------------|---------|
| BRCA | 14 | 0 | 2 |
| KIRC | 953 | 894 | 96 |
| LUAD | 29 | 10 | 1 |

Table 2: Number of significant survival-related features per project and analyzed feature.

Surprisingly, the amount of significant features is clearly unbalanced between KIRC and the other two cancers. Notice that statistics show that KIRC has generally a better prognosis than another types of cancer, contributing with a meager 1.1% deaths related by cancer worldwide in comparison with the 18.4% related to LUAD [1].

Unfortunately, we found no common survival-related features significant in all three cancers at the same time. However, a number of survival-related features common to two of the three cancers were found: 31 subpathways, 6 Gene Ontology functions and 3 Uniprot keywords. Figure 4B shows the number of survival-related paths shared by each pair of cancer projects by means of an UpSet plot [18].

Among the pairwise common survival-related paths we find subpathway *AMPK signaling pathway: CCNA2*, which was commonly up-regulated along the three cancers (see Section *Common & Specific features* and Figure 3). This subpathway has been significantly related to survival in KIRC and LUAD. In both cancers, a higher activity of this pathway is related to a poorer outcome, and a lower activity of the pathway is linked to a better outcome. Figure 4C shows the Kaplan-Meier curves for the three groups (20% of higher values in red, 20% of lower values in blue and remaining 60% of values in orange) in KIRC (top) and LUAD (bottom).

Conclusions

Cancer is an extremely complicated and heterogeneous disease, in which the gene-centric approach has proven to need a wider point of view to be able to explain all the changes arising in a cancer cell and its microenvironment. Biology-based models which take into account the topology of the protein interactions and allow to interpret cell function in this way arise as a novel approach in the analysis of cancer.

Initiatives as the CAMDA 2019 Hi-Res Cancer Data Integration Challenge are a great opportunity to analyze curated data from different technologies and projects. In this work we departed from the gene expression data of breast, kidney and lung cancers and applied the Hipathia methodology to estimate the levels of activity of 1868 subpaths, 1654 Gene Ontology functions and 142 Uniprot keywords and find hidden patterns of functional activity.

The joint analysis of these different cancer datasets reported an appreciable number of common functional features which in turn can be linked to specific cancer hallmarks, suggesting a common carcinogenic process unrelated to the tumor tissue of origin. Interestingly, some of these pathways and functions were at the same time related to survival in two of the three analyzed cancers. Since the three cancers are adenocarcinomas, a shared cell origin may be at the core of the similarities.

On the other hand, tumor-specific pathways and functions have been determined, allowing a better understanding of the specificity of each cancer, and how the processes leading to disease may be different in each of the tissues.

Materials And Methods

Data download and normalization

Data provided for the CAMDA 2019 Hi-Res Cancer Data Integration Challenge was downloaded from the SFTP server hosted at BOKU Vienna. Local copies of the processed data publicly available from the GDC corresponding to matched gene expression values were used for this work. Data came from 3 different cancer projects: breast cancer (TCGA-BRCA project, with 656 samples, corresponding to 589 Primary Tumor samples and 67 Solid Tissue Normal samples), kidney cancer (TCGA-KIRC project, with 602 samples, corresponding to 530 Primary Tumor samples and 72 Solid Tissue Normal samples) and lung adenocarcinoma (TCGA-LUAD project, with 574 samples, corresponding to 515 Primary Tumor samples and 59 Solid Tissue Normal samples). RNA-Seq data was subsequently normalized with TMM normalization [19] and log transformed.

Pathway & functional level computation

The matrix of normalized gene expression was scaled between 0 and 1, and transformed to a matrix of pathway activation values by means of the *Hipathia* Bioconductor package [12]. This methodology computes a score representing the activity of each of the analyzed effector subpathways from the gene expression data by means of an iterative algorithm. An effector subpathway (from now on, *subpathway*) includes any node in a subpathway ending in a particular effector protein, and determines the joint activity arriving to it. Hipathia uses the information from the Kyoto Encyclopedia of Genes and Genomes (KEGG) [20] as layout for the topology of the pathways. From the matrix of pathway activities two new matrices of functional activities corresponding to Gene Ontology functions and Uniprot keywords were computed with the same package, taking into account the different pathways related to each one of the functions. A total of 1868 paths (from 146 KEGG signaling pathways), 1654 Gene Ontology functions and 142 Uniprot Keywords were analyzed.

Tumor vs. normal tissue comparisons

For each cancer type (project), a comparison between the gene, pathway and functional activation levels of the “Solid Tissue Normal” and “Primary Tumor” classes was performed with the Limma package [21]. The FDR [22] correction method was used to adjust the multiple testing effects on the *p-values*, and a cutoff of $\alpha = 0.05$ was established to determine statistical significance. Heatmaps with the features with a significant *p-value* and an absolute value of the logarithm of the Fold Change (logFC) greater than 0.3 were plotted, allowing a non-supervised clustering method to establish the order for the rows and columns by similarity.

Common & specific results

Common results at a subpathway and function level were established by selecting the features (pathways and functions separately) with a) statistical significance in the tumor vs. normal tissue

comparisons in all three projects, and b) common sign of the logFC in all three projects. Same sign of the logFC assures that the significant changes are always in the same direction (up or down activated). Cancer specific results were established by selecting those features which were statistically significant just in one of the analyzed cancers.

Survival-related pathways and functions

For each analyzed feature, samples were divided into three groups: 20% of most activated samples, 20% of lowest activated samples and the 60% of remaining samples. An analysis including function *survdiff* from the *survival* R package [23] was performed on each feature, which returns a Chi-squared statistic which is used to calculate a *p-value*. The FDR method [22] is used as above to correct for multiple testing effects. Kaplan - Meier curves [24] were plotted to visualize survival differences among the defined groups. Pairwise common survival-related features were established by selecting those with a significant *p-value* in two different projects at the same time. UpSet plots [18] representing the number of overlapping survival-related pathways or functions were created with package *UpSetR* [25].

Declarations

- **Ethics approval and consent to participate**

Not applicable.

- **Consent for publication**

Not applicable.

- **Availability of data and materials**

The datasets analysed during the current study are available in the GDC Data Portal repository, <http://gdc.cancer.gov>.

- **Competing interests**

The authors declare that they have no competing interests.

- **Funding**

This study was co-funded by the European Regional Development Funds (FEDER) in the Valencian Community 2014-2020 and the Principe Felipe Research Center fundings from the Conselleria de Sanitat of the Generalitat Valenciana, Spain.

- **Authors' contributions**

SRG assisted in the analysis of the data, interpreted the results in a cancer context and helped in the development of the manuscript. FGG supervised the analysis performed and helped in the development of the manuscript. MRH analyzed the data and was a major contributor in writing the manuscript. All authors read and approved the final manuscript.

- **Acknowledgements**

Principe Felipe Research Center for providing access to the cluster, co-funded by European Regional Development Funds (FEDER). Authors want to acknowledge also all participants in the CAMDA 2020 COSI for sharing their ideas and comments.

- **Author information**

Sergio Romera-Giner: sergio.romera@atos.net

Francisco Garcia-Garcia: fgarcia@cipf.es

Marta R. Hidalgo: mhidalgo@cipf.es

References

1. Bray F, Ferlay J, Sorjomataram I, Siegel R, Torre LA, Jemal A. Global Cancer Statistics 2018: GLOBOCAN Estimates of Incidence and Mortality Worldwide for 36 Cancers in 185 Countries. *CA Cancer J Clin* 2018;68(6):394-424. doi: 10.3322/caac.21492
2. Hanahan D, Weinberg R. The Hallmarks of Cancer. *Cell* 2000;100:57-70. doi: 10.1016/s0092-8674(00)81683-9
3. Hanahan D, Weingberg RA. Hallmarks of Cancer: The Next Generation. *Cell* 2011;144:646-674. doi:10.1016/j.cell.2011.02.013
4. Jonsson P, Bandlamudi C, Cheng ML, Srinivasan P, Chavan SS, Friedman ND, et al. Tumour lineage shapes BRCA-mediated phenotypes. *Nat.* 2019;571:576-579. doi: 10.1038/s41586-019-1382-1
5. Malvia S, Bagadi SAR, Pradhan D, Chintamani C, Bhatnagar A, Arora D, Sarin R, Saxena S. Study of Gene Expression Profiles of Breast Cancers in Indian Women, *Sci Rep.* 2019;9:10018. doi: 10.1038/s41598-019-46261-1
6. Ali, HEA, Lung PY, Sholl AB, Gad SA, Bustamante JJ, Ali HI, Rhim JS, Deep G, Zhang J, Abd Elmageed ZY. Dysregulated gene expression predicts tumor aggressiveness in African-American prostate cancer patients. *Sci Rep.* 2018; doi: 10.1038/s41598-018-34637-8
7. Xu T, Le TD, Liu L, Su N, Wang R, Sun B, Colaprico A, Bontempi G, Li J. CancerSubtypes: an R/Bioconductor package for molecular cancer subtype identification, validation, and visualization. *Bioinf.* 2017; doi: 10.1093/bioinformatics/btx378.
8. Dalakas MC. Mechanisms of Disease: signaling pathways and immunobiology of inflammatory myopathies. *Nat Clin Prac Rheu.* 2006; doi: 10.1038/ncprheum0140

9. Mueller KA, Glajch KE, Huizenga MN, Wilson RA, Granucci EJ, Dios AM, et al. Hippo Signaling Pathway Dysregulation in Human Huntington's Disease Brain and Neuronal Stem Cells. *Sci Rep*. 2018; doi: 10.1038/s41598-018-29319-4.
10. Escors D, Gato-Cañas M, Zuazo M, Arasanz H, García-Granda MJ, Vera R, Kochan G. The intracellular signalosome of PD-L1 in cancer cells. *Sig Trans and Targ Th*. 2018; doi: 10.1038/s41392-018-0022-9
11. Tian T, Li X, Zhang J. mTOR Signaling in Cancer and mTOR Inhibitors in Solid Tumor Targeting Therapy. *Int J Mol Sci*. 2019; doi: 10.3390/ijms20030755.
12. Hidalgo MR, Cubuk C, Amadoz A, Salavert F, Carbonell-Caballero J, Dopazo J. High throughput estimation of functional cell activities reveals disease mechanisms and predicts relevant clinical outcomes. *Oncotarget*. 2017; doi: 10.18632/oncotarget.14107.
13. Amadoz A, Hidalgo MR, Çubuk C, Carbonell-Caballero J, Dopazo J. A comparison of mechanistic signaling pathway activity analysis methods, *Brief in Bioinf*. 2018; doi: 10.1093/bib/bby040
14. Grossman RL, Heath AP, Ferretti V, Varmus HE, Lowy DR, Kibbe WA, Staudt LM. Toward a Shared Vision for Cancer Genomic Data. *N Eng J Med*. 2016; 375(12):1109-1112
15. Clark K, Vendt B, Smith K, Freyman J, Kirby J, Koppel P, et al. The Cancer Imaging Archive (TCIA): Maintaining and Operating a Public Information Repository. *J Digit Imaging*. 2013;26(6):1045-1057. doi: 10.1007/s10278-013-9622-7
16. Yuen GJ, Demissie E, Pillai S. B lymphocytes and cancer: a love-hate relationship. *Trends Cancer*. 2016;2(12):747-757. doi: 10.1016/j.trecan.2016.10.010
17. Lastraioli E, Iorio J, Arcangeli A. IOn channel expression as promising cancer biomarker. *Biochim Biophys Acta*. 2015;1848(10 Pt B): 2685-702. doi: 10.1016/j.bbame.2014.12.016.
18. Lex A, Gehlenborg N, Strobel H, Vuillemot R, Pfister H. UpSet: Visualization of Intersecting Sets. 2014. *IEEE Trans Vis Comput Graph*. 2014; 20(12):1983–1992. doi: 10.1109/TVCG.2014.2346248
19. Robinson MD, Oshlack A. A scaling normalization method for differential expression analysis of RNA-seq data. 2010. *Gen Bio*. doi: 10.1186/gb-2010-11-3-r25
20. Kanehisa, M. and Goto, S. KEGG: Kyoto Encyclopedia of Genes and Genomes. *Nuc Ac Res*. 2000;28:27-30. Doi: 10.1093/nar/28.1.27
21. Ritchie ME, Phipson B, Wu D, Hu Y, Law CW, Shi W, Smyth GK. limma powers differential expression analyses for RNA-sequencing and microarray studies. *Nuc Ac Res*. 2015; doi: 10.1093/nar/gkv007.
22. Benjamini Y, Hochberg Y. Controlling the False Discovery Rate: A Practical and Powerful Approach to Multiple Testing. *J Roy Stat Soc. Series B (Methodological)*. 1995;57(1):289-300.
23. Therneau TM, Grambsch PM. *Modeling Survival Data: Extending the Cox Model*. New York: Springer; 2000.
24. Kaplan E, Meier P. Nonparametric estimation from incomplete observations. *J Am Stat Assoc*. 1958;53(282):457–481. doi: 10.1080/01621459.1958.10501452
25. Conway JR, Lex A, Gehlenborg N. UpSetR: an R package for the visualization of intersecting sets and their properties. *Bioinf*. 2017;33(18):2938–2940, doi: 10.1093/bioinformatics/btx364

Figures

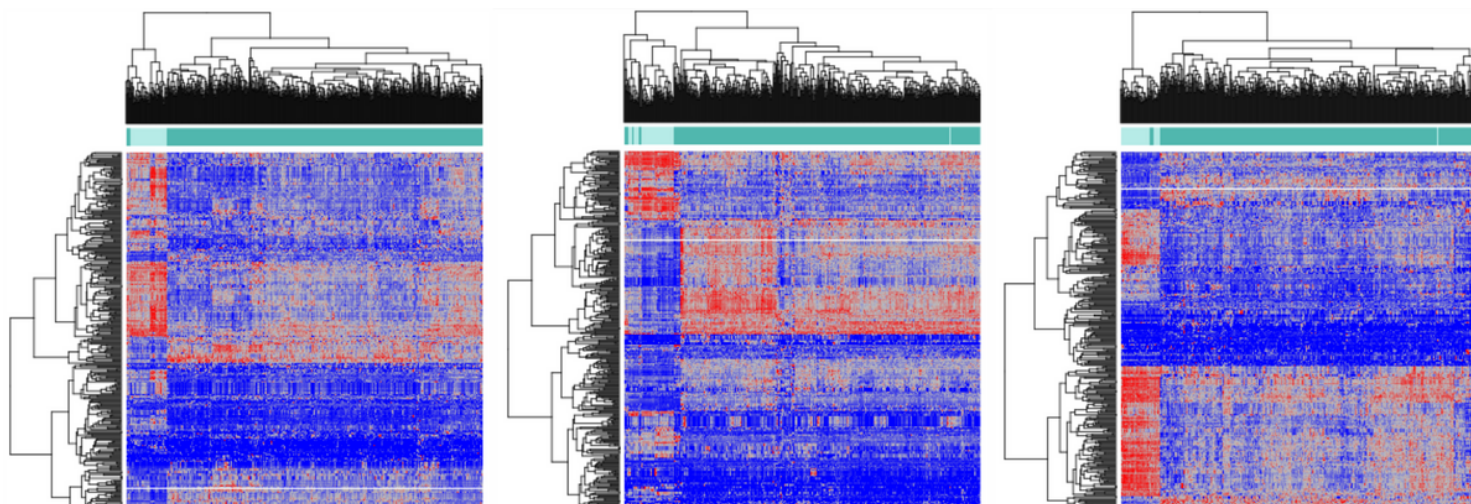


Figure 1

Heatmaps of effector subpathways activity. Samples and paths were ordered following the results of a non-supervised clusterization. Left: BRCA cancer data. Center: KIRC cancer data. Right: LUAD cancer data.

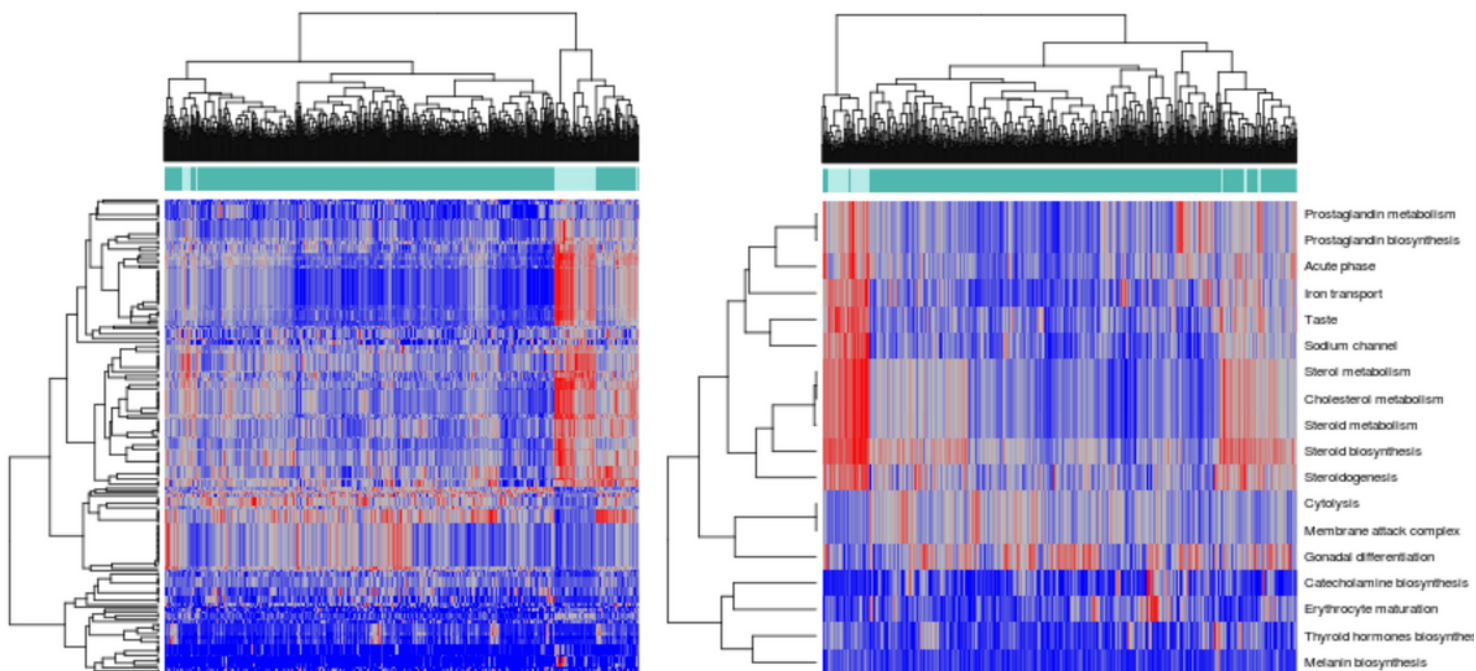


Figure 2

Heatmaps of function activations in BRCA cancer. Samples and functions were ordered following the results of a non-supervised clusterization. Left: Gene Ontology functions. Right: Uniprot keywords.

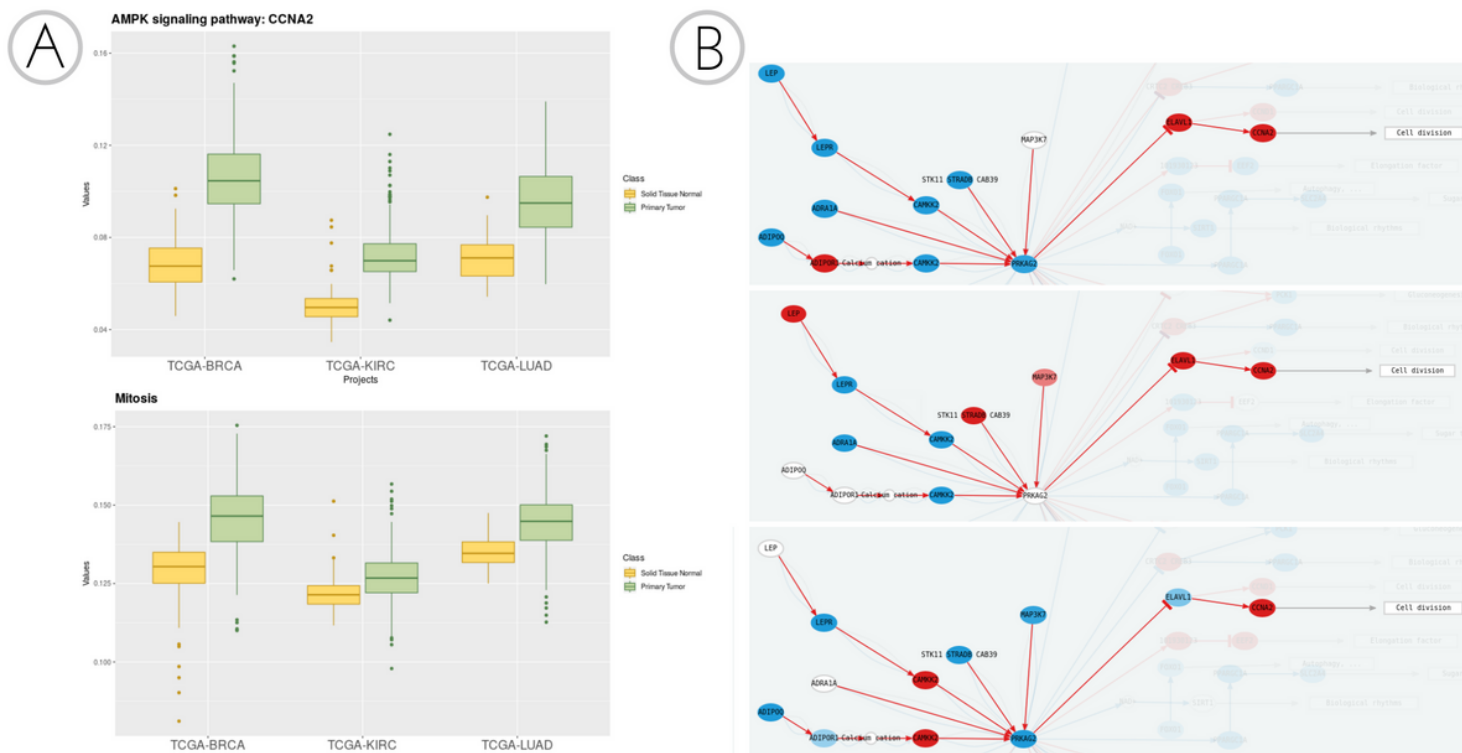


Figure 3

A) Boxplots representing the distribution of the activity values for the AMPK signaling pathway: CCNA2 subpathway (top) and the Uniprot keyword Mitosis (bottom). Expression values are grouped by tissue type (tumor or normal) and cancer. B) Up and down regulation of genes in the AMPK signaling pathway: CCNA2 subpathway in BRCA (top), LUAD (center) and KIRC (bottom). Blue nodes correspond to significant down-regulated genes, red nodes correspond to significant up-regulated genes and white nodes correspond to non-significant nodes. Red lines are depicted because the whole activity of the pathway is significantly up-activated after an statistical analysis.

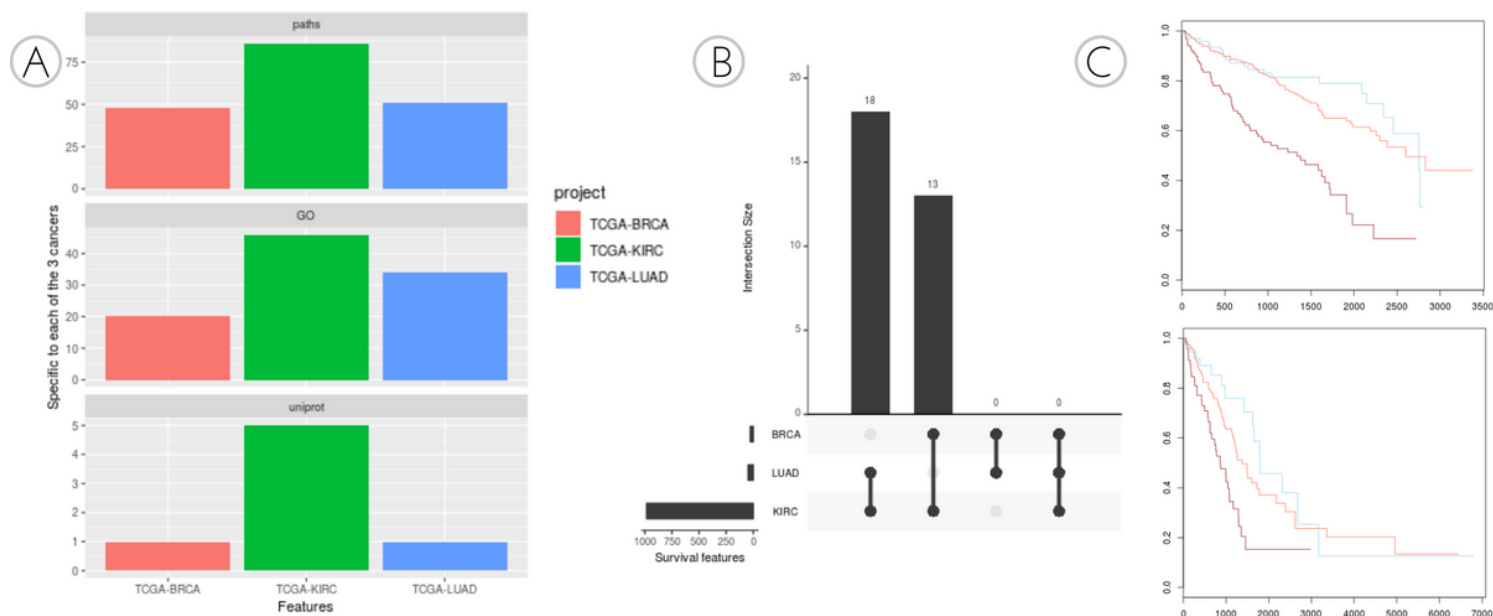


Figure 4

A) Number of specific features per cancer. B) UpSet plot indicating the number of paths in the pairwise intersections among the three analyzed cancers, and the (null) intersection of the three of them. C) Kaplan-Meier curves for the three groups of activation intensity defined by subpathway AMPK signaling pathway: CCNA2 in KIRC (top) and LUAD (bottom). Blue lines correspond to the 20% of samples with lowest activity values, red lines correspond to the 20% of samples with highest activity values of this pathway and orange lines correspond to the remaining 60% of samples.

Supplementary Files

This is a list of supplementary files associated with this preprint. Click to download.

- [TableS2CommonfeaturesGOnoFC.xls](#)
- [TableS1CommonfeaturespathsnoFC.xls](#)
- [TableS4SpecificfeaturespathsnoFC.xls](#)
- [TableS3CommonfeaturesuniprotnoFC.xls](#)
- [TableS5SpecificfeaturesGOnoFC.xls](#)
- [TableS6SpecificfeaturesuniprotnoFC.xls](#)